


Deciphering the promiscuous interactions between intrinsically disordered transactivation domains and the KIX domain

Yongqi Huang^{1,2,3,4}  | Meng Gao^{1,2,3,4} | Fei Yang^{1,2,3,4} | Lei Zhang^{1,2,3,4} | Zhengding Su^{1,2,3,4}

¹Institute of Biomedical and Pharmaceutical Sciences, Hubei University of Technology, Wuhan, China

²Key Laboratory of Fermentation Engineering (Ministry of Education), Hubei University of Technology, Wuhan, China

³Hubei Key Laboratory of Industrial Microbiology, Hubei University of Technology, Wuhan, China

⁴Hubei Collaborative Innovation Center for Industrial Fermentation, Hubei University of Technology, Wuhan, China

Correspondence

Yongqi Huang and Zhengding Su
Department of Biological Engineering,
Hubei University of Technology, Wuhan,
Hubei, 430068 China. Emails:
yqhuang@pku.edu.cn and zhengding.
su@mail.hbut.edu.cn

Funding information

National Natural Science Foundation of China (Y.H.), Grant/Award Number: 21603121; Wuhan Natural Science Foundation (Z.S.), Grant/Award Number: 201506101010033, Hubei University of Technology (Y.H. and Z.S.)

Abstract

The kinase-inducible domain interacting (KIX) domain of the transcriptional coactivator CBP protein carries 2 isolated binding sites (designated as the c-Myb site and the MLL site) and is capable of binding numerous intrinsically disordered transactivation domains (TADs), including c-Myb and pKID via the c-Myb site, and MLL, E2A and c-Jun via the MLL site. In this study we compared the kinetics for binding of various disordered TADs to the KIX domain via computational biophysical analyses. We found that the binding rates are heavily affected by long-range electrostatic interactions. The basal rate constants for forming the encounter complexes are similar for different KIX binding peptides, favorable electrostatic interactions between the MLL site and the peptides result in greater association rates when peptides bind to the MLL site. FOXO3a and p53 TAD each contains 2 copies of KIX binding motif and each motif interacts with both the MLL site and the c-Myb site. Our kinetics studies suggest that binding of FOXO3a or p53 TAD to the KIX domain is via a sequential mechanism, where one KIX binding motif binds to the MLL site first and then the other KIX binding motif binds to the c-Myb site. Considering the promiscuous interactions between FOXO3a and KIX, and p53 TAD and KIX, electrostatic steering simplifies the binding mechanism. This study highlights the importance of long-range electrostatic interactions in molecular recognition process involving multi-motif intrinsically disordered proteins and promiscuous interactions.

KEYWORDS

binding mechanism, electrostatic steering effect, intrinsically disordered proteins, protein–protein interaction, sequential binding

1 | INTRODUCTION

Although many proteins fold into well-defined 3 dimensional structures to perform their biological functions, around 30% of the proteome are functional disordered proteins.^{1,2} These intrinsically disordered proteins (IDPs) are widely involved in cellular processes. Bioinformatics studies have shown that IDPs are enriched in cellular functions related to signal transduction and molecular recognition.^{3,4} It is now accepted that the lack of structure in IDPs is fundamental to their functions.^{5–8}

IDPs interact with their targets via short segments called recognition motifs.⁹ The motif-based modular structure of IDPs enables different IDPs or different segments of an IDP to interact with a common target. One of such versatile targets is the kinase-inducible domain interacting (KIX) domain of the transcriptional coactivator CBP protein. The KIX domain contains 2 isolated binding sites (designated as the

c-Myb site and the MLL site) and is able to bind to numerous intrinsically disordered transactivation domains (TADs) carrying the “ΦXXΦΦ” motif, where “Φ” is a hydrophobic residue, and “X” is an arbitrary residue (Figure 1A). The TADs of CREB (pKID) and c-Myb bind to the c-Myb site of KIX, while the TADs of MLL, E2A, and c-Jun bind to the MLL site of KIX (Figure 1B).^{10–13} Since the 2 binding sites of the KIX domain are isolated, one KIX domain is capable of binding 2 disordered TADs simultaneously, where one TAD binds to the c-Myb site and the other one binds to the MLL site.^{11,14–16}

Understanding the binding mechanism is critical to understand how disordered transcription factors perform their functions. Binding mechanisms for the interaction of KIX with pKID and the interaction of KIX with c-Myb have been characterized extensively.^{17–20} It is found that binding of pKID to KIX is via an induced-fit mechanism and binding of c-Myb to KIX is via a combination of conformational selection



FIGURE 1 Interactions between disordered TADs and the KIX domain. A, Sequence alignment of the KIX binding TADs. Residues in the conserved “ΦXXΦΦ” motif are highlighted in red. B, Structures of KIX in complex with c-Myb and MLL (PDB: 2AGH). The KIX domain is shown in blue, the c-Myb is shown in orange, and the MLL is shown in green

and induced-fit mechanisms.¹⁹ Interactions between a disordered TAD and the KIX domain will become more complicated when the disordered TAD contains more than one copy of the KIX binding motif, such as the TADs of p53 and the Forkhead box class O 3a (FOXO3a) (Figure 1A). The p53 TAD consists of 2 subdomains (AD1 and AD2). NMR characterization showed that the AD1 and AD2 subdomains each interact with both the MLL site and the c-Myb site when p53 TAD associates with the KIX domain.²¹ Similarly, promiscuous interactions were also observed in the interactions between FOXO3a and KIX, where the CR2C and CR3 segments of FOXO3a interact with the KIX domain at both the MLL site and the c-Myb site.²²

Coupled folding and binding is a general mechanism to describe the interactions between IDPs and their targets.²³ Recently, Zhou et al.²⁴ introduced the sequential binding element into the coupled folding and binding mechanism and proposed a dock-and-coalesce framework to describe binding processes involving multi-segment IDPs, where one segment of the IDP first docks to its subsite on the target surface and the remaining segments subsequently coalesce around their respective subsites. The promiscuous interactions between FOXO3a and KIX and between p53 TAD and KIX complicate the binding mechanism of these 2 complexes and their binding mechanisms have not been studied so far.

In this work, we investigated the mechanisms of FOXO3a binding to KIX and p53 TAD binding to KIX via computational biophysical analyses. Our results revealed a common kinetic feature for interactions between disordered TADs and the KIX domain, where binding of TADs to the MLL site is electrostatically more favorable and faster than binding of TADs to the c-Myb site. Our results suggest a sequential binding mechanism to account for the association of dual-motif transcription factors FOXO3a and p53 TAD with KIX, where one motif binds to the MLL site first and then the other motif binds to the c-Myb site.

2 | MATERIALS AND METHODS

2.1 | Protein complexes studied

The disordered TAD/KIX complexes studied in this work were: pKID/KIX (PDB: 1KDX), c-Myb/KIX (PDB: 1SB0), MLL/KIX (PDB: 2LXS), E2A/KIX (PDB: 2KWF), FOXO3a/KIX (PDB: 2LQH and 2LQI), and p53 TAD/KIX. The structures for the p53 TAD/KIX complex were generated by homology modeling as described below.

Structure models of the p53 TAD/KIX complex were generated by the Modeller 9.16 program.²⁵ The NMR structures of the FOXO3a/KIX complex (PDB: 2LQH and 2LQI) were used as templates with p53 AD1 subdomain aligning with FOXO3a CR2C segment and p53 AD2 subdomain aligning with FOXO3a CR3 segment (Figure 1). Corresponding to the dual conformations of the FOXO3a/KIX complex, 2 conformations were generated for the p53 TAD/KIX complex: in one conformation, p53 AD1 binds to the c-Myb site and p53 AD2 binds to the MLL site; in the other conformation, p53 AD1 binds to the MLL site and p53 AD2 binds to the c-Myb site. The structure models for the p53 TAD/KIX complex were then relaxed by energy minimization and 10 ns molecular dynamics (MD) simulations using Gromacs 4.5.4²⁶ and Amber force field²⁷ at 298 K and 1 bar.

2.2 | Association rate constants calculation

Based on the transient complex theory,²⁸ Zhou et al. developed the TransComp method to predict the association rates for protein–protein interactions²⁹ and understand the binding mechanisms of IDPs.^{30–32} According to the transient complex theory, the association rate constant for a diffusion-limited binding process is expressed as $k_a = k_{a0} \exp(-\Delta G_{el}^*/k_B T)$, where k_{a0} is the basal rate constant for forming the transient complex via random diffusion, and ΔG_{el}^* is the electrostatic interaction energy of the transient complex.²⁸ Association rate constant calculation was carried out via the TransComp server (<http://pipe.sc.fsu.edu/transcomp/>) which requires only the structure of the native complex as input and automatically performs the simulations and data analysis. The TransComp calculation consists of 3 steps. The first step is to determine the transient complex by analyzing the energy landscape of the interacting proteins. In the native complex energy well, the number of native contacts, N_c , between the 2 proteins is large, but the standard deviation, σ_χ , in the rotation angle χ is small. As the 2 proteins move out of the native complex well, σ_χ sharply increases and N_c sharply decreases. The dependence of σ_χ on N_c is fitted to a 2-state transition function and the transient complex is identified as the midpoint of the transition. Once the transient complex is determined, k_{a0} is calculated from force-free Brownian dynamics simulations. The third step is to calculate the electrostatic interaction energy ΔG_{el}^* for the transient complex, by solving the Poisson-Boltzmann equation. The ionic strength was set to 0.15 M in the electrostatic interaction energy calculations.

TABLE 1 Association rate constants for binding of single motif peptides to the KIX domain

Binding site	Peptide	Calculated			Experimental ^a k_a ($\mu\text{M}^{-1}\text{s}^{-1}$)
		k_{a0} ($\mu\text{M}^{-1}\text{s}^{-1}$)	ΔG_{el}^* (kcal/mol)	k_a ($\mu\text{M}^{-1}\text{s}^{-1}$)	
c-Myb	c-Myb	0.86	-0.38	1.64	8.1
	pKID	0.29	-1.25	2.39	5.0
MLL	MLL	Not a single-step process			39
	E2A	Not a single-step process			57

^aData from reference.³⁹

2.3 | Coarse-grained MDs simulations

Topology-based MDs simulations were performed to study the binding mechanism of FOXO3a with the KIX domain. The C_α -only Gō-like model³³ was adopted to describe the interactions, where a protein was represented by the C_α atoms. The first NMR model of each binding mode (PDB 2LQH for the 2b3I-binding mode and PDB 2LQI for the 2I3b binding mode) was used to represent the structure of FOXO3a/KIX complex. Interactions for residue pairs forming native contacts were described by a 12–10 Lennard-Jones potential form.³⁴ Interaction strength was set to 1.0 ϵ for interactions within FOXO3a and interactions between FOXO3a and KIX and 2.0 ϵ for interactions within the KIX domain. To reduce the influence of the loop region between CR2C and CR3 segments on the binding process, interaction strength for residue pairs involving the loop region was set to 0.5 ϵ . Electrostatic interactions were modeled using the Debye-Hückel potential.³⁵ The dielectric constant was set to 80 and ionic strength was set to 0.15 M. Other parameters were set as in references.^{36,37}

Langevin dynamics was used to perform the simulations. Simulations were conducted by placing a FOXO3a peptide and a KIX domain in a 150 Å cubic box. Periodic boundary conditions were applied in all 3 directions. Free energy profiles were calculated from simulations with bias potentials.³⁸ The fraction of native intermolecular contacts (Q_b) was used to monitor the binding/unbinding process and used as the reaction coordinate to describe the free energy profiles. Free energy (G) was calculated as $G(Q_b)/k_B T = -\ln[P(Q_b)]$, where k_B is the Boltzmann constant, $P(Q_b)$ is the probability distribution of Q_b . The unbound state was defined as conformations with $Q_b = 0$ and the bound state was defined as conformations with $Q_b \geq 0.7$. The encounter complex was defined as conformations with one native intermolecular contact. The transition temperature T_m was defined as the temperature under which the unbound state and the bound state had equal probability. Production simulations were then performed at T_m to sample the bound and unbound states with similar probabilities. 200 binding/unbinding transitions were simulated to analyze the formation and evolution of encounter complexes.

3 | RESULTS

3.1 | Binding kinetics for KIX with single-motif TADs

KIX interacts with c-Myb and pKID via the c-Myb site, and with MLL and E2A via the MLL site (Figure 1B). The binding kinetics of these

single motif TADs with the KIX domain has been characterized systematically by stopped-flow technique.³⁹ Binding of TAD peptides to the KIX domain is fast with basal rate constants in the order of $\mu\text{M}^{-1}\text{s}^{-1}$ and the binding process is enhanced by favorable long-range electrostatic interactions. Further analysis indicated that the binding process is diffusion-limited.³⁹

Here, the binding kinetics for the KIX domain with different TAD peptides was analyzed by the TransComp method (Table 1). The predicted basal rate constants for binding of c-Myb and pKID to the KIX domain were 0.86 and 0.29 $\mu\text{M}^{-1}\text{s}^{-1}$, which were an order of magnitude smaller than the experimental results.³⁹ Although the TransComp method underestimated the basal rate constants, the favorable long-range electrostatic interactions were captured in the TransComp calculations and the predicted binding rate constants were in agreement with experimental values. For example, the predicted binding rate for c-Myb/KIX interaction was 1.64 $\mu\text{M}^{-1}\text{s}^{-1}$ and the experimental determined value was 8.1 $\mu\text{M}^{-1}\text{s}^{-1}$. For pKID/KIX interaction, the predicted binding rate was 2.39 $\mu\text{M}^{-1}\text{s}^{-1}$ and the experimental determined value was 5.0 $\mu\text{M}^{-1}\text{s}^{-1}$ (Table 1).

Although the rank order of the predicted binding rates was different from that of the experimentally determined binding rates, the predicted binding rates were in a similar order of magnitude to the experimental values. There could be several reasons for this discrepancy. One could be that TransComp method assumes association of 2 folded domains. The effect of intrinsically structural disorder on binding kinetics has been extensively studied in the past decade, and it is generally found that structural disorder could increase the binding rate but with a subtle effect.⁶ Usually, the enhancement of binding rate resulted from intrinsic disorder is about 2–3 folds.^{38,40,41} On the other hand, the uncertainty of TransComp prediction could be as large as 30 folds.²⁹ Therefore, assuming that intrinsically disordered binding segments acquire folded structures prior to binding is reasonable in the TransComp calculation for protein complexes involving IDPs.

Unlike c-Myb and pKID, TransComp calculations showed that binding of MLL and E2A peptides (with various length) to the MLL site of KIX domain may be more complicated than a docking process and thus the binding rates could not be calculated for these 2 KIX binding peptides.

3.2 | Binding kinetics for KIX with dual-motif TADs

FOXO3a contains 2 KIX-binding motifs, that is, the CR2C segment and CR3 segment. Through these 2 segments, FOXO3a simultaneously

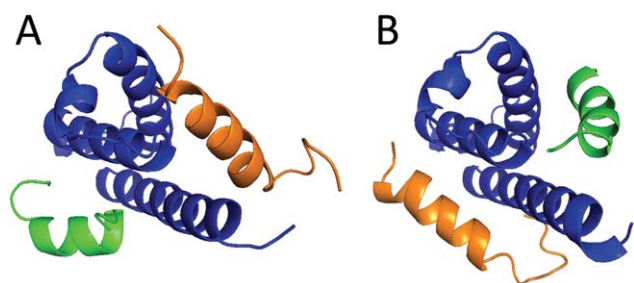


FIGURE 2 Structures of FOXO3a in complex with KIX via the 2l3b mode (A) and the 2b3l mode (B). The KIX domain is shown in blue; the CR2C segment is shown in orange and the CR3 is in green. The linker connecting the CR2C and CR3 segments is not shown for clarity [Color figure can be viewed at wileyonlinelibrary.com]

binds to the c-Myb site and the MLL site of the KIX domain, resulting in 2 modes of association: in one mode, CR2C binds to the MLL site and CR3 binds to the c-Myb site (the 2l3b mode); in the other mode, CR3 binds to the MLL site and CR2C binds to the c-Myb site (the 2b3l mode) (Figure 2).²² TransComp calculations predicted that the basal rate constants for the binding of CR2C and CR3 peptides to the KIX domain were in sub $\mu\text{M}^{-1} \text{s}^{-1}$ range and were similar to other KIX binding peptides (Table 2). Most importantly, we found that binding of FOXO3a peptides to the MLL site was much faster (about 40 folds) than binding of FOXO3a peptides to the c-Myb site (Table 2). Actually, binding of MLL and E2A to the MLL site were also faster than binding of pKID and c-Myb to the c-Myb site (Table 1).

The predicted basal rate constants for binding of peptides to the c-Myb site were rather similar to those for the MLL site (Tables 1 and 2). Interestingly, the predicted electrostatic interactions for the MLL site were much more favorable than those for the c-Myb site (Table 2). The electrostatic interaction energy ΔG_{el}^* were -0.502 and 0.467 kcal/mol for binding of FOXO3a peptides to the c-Myb site and were -2.39 and -2.18 kcal/mol for binding of FOXO3a peptides to the MLL site. From the electrostatic potential surface of the KIX domain, we found that the MLL site was more positively charged than the c-Myb site (Figure 3). Since the “ $\Phi\text{XX}\Phi\Phi$ ” motif is surrounded by negatively charged residues (Figure 1), the favorable electrostatic interactions between the MLL site and the negatively charged residues may steer the conformational search process and enhance the association.

Interactions between p53 TAD and the KIX domain have been characterized by NMR. The p53 AD1 and AD2 subdomains were found

TABLE 2 Predicted association rate constants for binding of FOXO3a peptides to the KIX domain

Binding site	Peptide	$k_{\text{a}0}$ ($\mu\text{M}^{-1}\text{s}^{-1}$)	ΔG_{el}^* (kcal/mol)	k_{a} ($\mu\text{M}^{-1}\text{s}^{-1}$)
c-Myb	CR2C	0.22	-0.502	0.51
	CR3	0.90	0.467	0.41
MLL	CR2C	0.39	-2.39	21.9
	CR3	0.35	-2.18	14.0

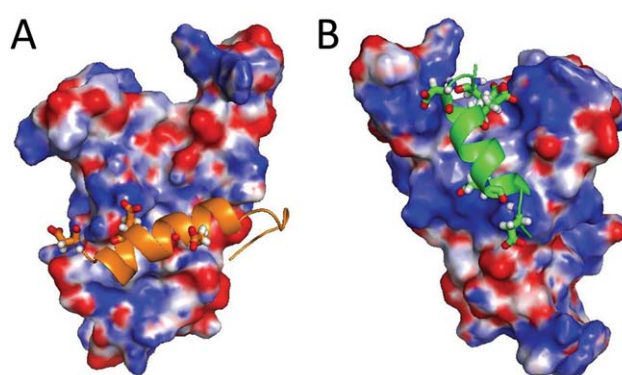


FIGURE 3 Electrostatic potential surface of the KIX domain. FOXO3a/KIX complex in the 2b3l binding mode is utilized to indicate the c-Myb site (A) and the MLL site (B), where the CR2C segment is shown in orange and the CR3 segment is shown in green. The negatively charged residues in FOXO3a are shown with sticks [Color figure can be viewed at wileyonlinelibrary.com]

to bind to both the c-Myb site and the MLL site.²¹ However, structures for the p53 TAD/KIX complex have not been determined so far. Since p53 TAD and FOXO3a show similar modes of interaction when they interact with the KIX domain individually, we used the structures of the FOXO3a/KIX complex to generate structure models for the p53 TAD/KIX complex. Corresponding to the 2 conformations of the FOXO3a/KIX complex, 2 conformations were generated for the p53 TAD/KIX complex: in one conformation the p53 AD1 subdomain binds to the c-Myb site and the AD2 subdomain binds to the MLL site; in the other conformation the AD1 subdomain binds to the MLL site and the AD2 subdomain binds to the c-Myb site. TransComp calculations were carried out with the proposed models for the p53 TAD/KIX complex. Similar to other KIX binding peptides, binding of p53 TAD peptides to the MLL site was faster than binding of p53 peptides to the c-Myb site due to favorable electrostatic interactions (Table 3).

3.3 | Topology-based modeling of FOXO3a binding to KIX

The TransComp method works for association processes limited by diffusion, including binding of single TAD motif to the KIX domain studied above. However, the TADs of FOXO3a and p53 each contains 2 copies of KIX-binding motif via a flexible linker. In this context, the TransComp method is not suitable to study the binding of dual-motif TADs to the KIX domain. Complementary to the TransComp calculation,

TABLE 3 Predicted association rate constants for binding of p53 peptides to the KIX domain

Binding site	Peptide	$k_{\text{a}0}$ ($\mu\text{M}^{-1}\text{s}^{-1}$)	ΔG_{el}^* (kcal/mol)	k_{a} ($\mu\text{M}^{-1}\text{s}^{-1}$)
c-Myb	AD1	0.91	-0.45	1.94
	AD2	0.78	0.09	0.66
MLL	AD1	0.93	-2.17	36.2
	AD2	0.30	-3.22	68.5

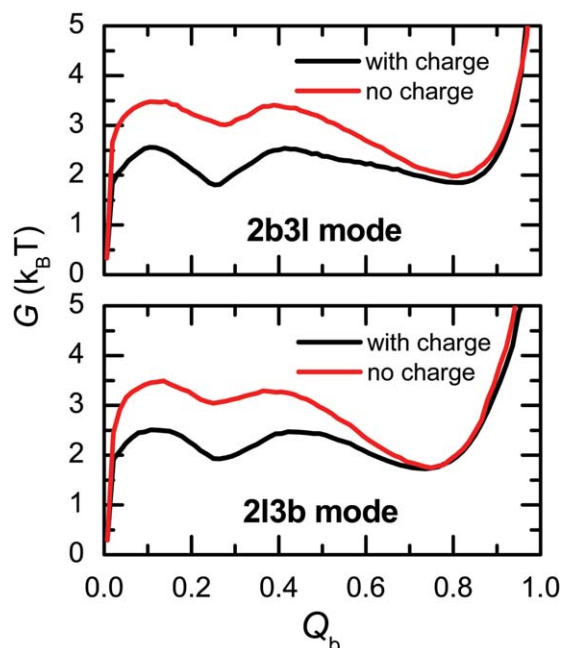


FIGURE 4 Free energy (G) as a function native intermolecular contact fraction (Q_b) at transition temperature T_m [Color figure can be viewed at wileyonlinelibrary.com]

structure-based coarse-grained MD simulations were performed to further characterize the binding process between FOXO3a and KIX. Simulations were based on the 2 structures of the FOXO3a/KIX complex. For both the 2l3b-binding mode and the 2b3l binding mode, the free energy profiles indicated that the free energy barriers were significantly reduced when electrostatic interactions were included in the simulations (Figure 4), which was consistent with the TransComp prediction.

The free energy profiles indicated that formation of the FOXO3a/KIX complex involving intermediate states, where about $\sim 25\%$ of native contacts between FOXO3a and KIX formed. Structural analysis on the ensemble of intermediate revealed that the FOXO3a predominantly docked to the c-Myb site when electrostatic interactions were

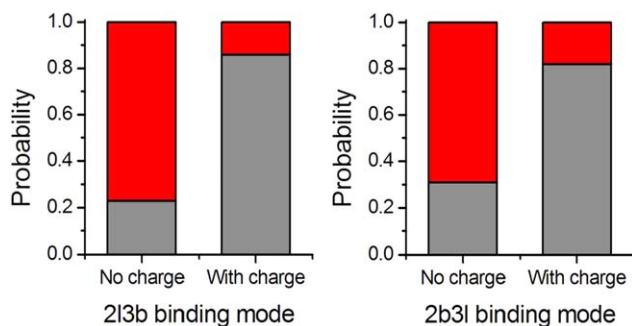


FIGURE 5 Docking of FOXO3a on the KIX surface in the intermediate state. The probabilities of CR2C and CR3 segments docking to the MLL site and c-Myb site were calculated from the simulated ensemble of intermediate state. Peptides docking to the MLL site and c-Myb site were shown in gray and red, respectively [Color figure can be viewed at wileyonlinelibrary.com]

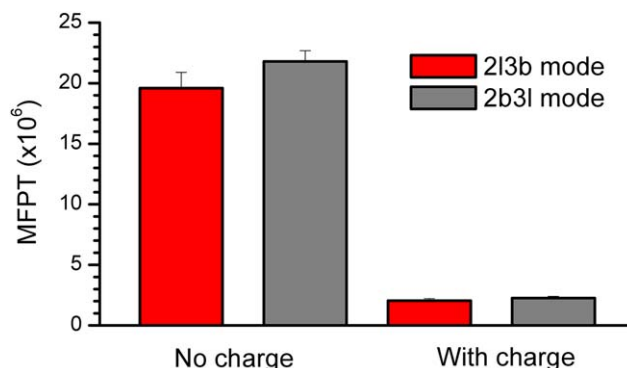


FIGURE 6 Kinetics of FOXO3a binding to KIX. Mean first passage time from the unbound state to the bound state was averaged from 200 binding events. The standard error was shown by the error bar [Color figure can be viewed at wileyonlinelibrary.com]

not included in the simulations (Figure 5). On the contrary, when electrostatic interactions were introduced, electrostatic steering biased the docking of FOXO3a to the MLL site (Figure 5). This feature indicated that electrostatic interactions could not only accelerate the binding rate but also remodel the binding mechanism.

Simulations under the transition temperature T_m enable us to simulate the binding/unbinding process reversibly (Supporting Information Figure S1) and calculate the binding rates. Consistent with the TransComp calculation, our coarse-grained simulations captured the accelerating effect of electrostatic interactions on the binding kinetics. Introducing electrostatic interactions enhanced the binding rate for about an order of magnitude (Figure 6). Our simulations revealed that the binding rates of the 2 binding modes were very similar, which is consistent with free energy landscape analysis above (Figure 4). We also calculated the binding rates for individual FOXO3a motif to the corresponding KIX binding site (Supporting Information Table S1). The simulated binding rates were consistent with the TransComp prediction in general trend (Supporting Information Figure S2).

The simulation trajectories were further examined in detail to reveal the influence of electrostatic interactions on the capture process, where encounter complexes formed. Without electrostatic interactions, the initial contacts between the 2 binding partners were highly promiscuous. FOXO3a showed similar probabilities to dock to the c-Myb site (0.56 for CR3 and 0.53 for CR2C) and the MLL site (0.47 for CR3 and 0.44 for CR2C) first (Figure 7A and Supporting Information Table S2). In contrast, with the inclusion of electrostatic interactions, docking of FOXO3a to KIX was biased. The probability of FOXO3a docking to the MLL site was dramatically increased (0.72 for CR3 and 0.84 for CR2C) (Figure 7A and Supporting Information Table S2), indicating a steering effect toward the MLL site. We further analyzed the evolution process (ie, from the encounter complexes to the native bound complex). Without electrostatic interactions, probability of productive encounter was small, around 0.1 (Figure 7B and Supporting Information Table S2). When electrostatic interactions were included in the simulation, the encounter complexes were stabilized and the probability of productive encounter was increased. This effect was more remarkable for the encounter complexes formed at the MLL site,

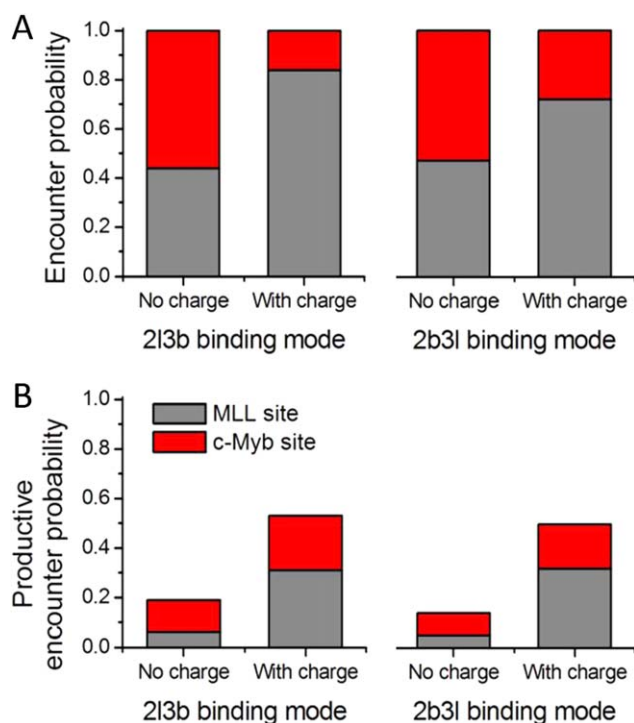


FIGURE 7 Probability of encounter complex formation between FOXO3a and KIX from simulations. (A) Probability of total encounter for the 2I3b and 2b3I binding modes. (B) Probability of productive encounter for the 2I3b and 2b3I binding modes. Encounter process triggered by the MLL site was shown by gray and encounter process triggered by the c-Myb site was shown by red [Color figure can be viewed at wileyonlinelibrary.com]

where the probability of productive encounter was increased by more than 5 folds (Figure 7B and Supporting Information Table S2). As a result, about 50% of the encounter process became productive in the presence of electrostatic interactions.

4 | DISCUSSION

Based on the transient complex theory, the TransComp method has been successfully applied to reproduce and predict the binding rates for various protein-protein complexes²⁹ and has recently been applied to study the binding mechanisms for IDPs.^{30–32} In this work, by applying the TransComp method, we investigated the binding kinetics for the KIX domain with several intrinsically disordered transcription factors. The predicted binding rates for the KIX domain with pKID and c-Myb via the c-Myb site, and with MLL and E2A via the MLL site agree well with the experimental values (Table 1).

Since FOXO3a and p53 TAD each contains 2 copies of KIX binding motif and each motif is able to interact with both the MLL site and the c-Myb site, 2 modes of interaction will be resulted when FOXO3a or p53 TAD associates with the KIX domain. For all KIX/peptide complexes studied here, the binding rates for interactions via the MLL site are faster than those for interactions via the c-Myb site. Our kinetics studies suggest that binding of FOXO3a or p53 TAD to the KIX domain is via a sequential mechanism, where one KIX binding motif

binds to the MLL site first and then the other KIX binding motif binds to the c-Myb site. It would be valuable to determine the overall binding rate constants for FOXO3a or p53 TAD to KIX as well as the binding rate constants for individual KIX binding motifs to KIX.

Sequential binding or dock-and-coalesce mechanism has been observed in many interacting processes involving multi-motif IDPs, for example, the p27/Cdk2/cyclin A complex,⁴² actin/actin-binding protein complexes,³⁰ and GTPase/effector complexes.³² Within a sequential binding process, the fast binding segment acts as the docking site which bind to the target and stabilize the binding intermediate. The intermediate state then evolves to the final bound state via binding of other segments and further conformation transitions. For interactions between FOXO3a and KIX and interactions between p53 TAD and KIX, the MLL site serves as the docking site and stabilizes the encounter complexes as revealed from our coarse-grained MD simulations (Figure 7).

Although sequential binding is the consequence of one motif binding faster than the others, the interplay or potential allosteric effect between multiple motifs may change the binding mechanism and sequential binding processes may not be observed in some circumstances. Comparing the overall binding mechanism of a multi-motif IDP with the binding mechanism of individual motif is needed to comprehensively understand the binding mechanism and the interplay between motifs. Therefore, combination of TransComp calculation and coarse-grained MDs simulation provides a more complete picture on the binding mechanism of multi-motif IDPs with their targets.

The predicted basal rate constants for forming the transient encounter complex are within similar range for all KIX/peptide interactions. Interestingly, we found that interactions between the peptide and the MLL site are electrostatically more favorable than interactions between the peptide and the c-Myb site. Favorable long-range electrostatic interactions have been found playing an important role in promoting the binding process of IDPs since the steering effect helps to align the ligand correctly on to the target surface.^{35,43–45} Although the interactions between FOXO3a and KIX or p53 TAD and KIX are promiscuous, electrostatic steering effects appear to simplify the binding mechanism by effectively guiding the initiation step via the MLL site.

5 | CONCLUSION

By performing theoretical kinetics analysis for the KIX domain with various disordered transcription factors, we found that the binding rates for KIX with its binding peptides are heavily affected by electrostatic interactions. The basal rate constants for forming the encounter complex are similar for various KIX binding peptides, favorable electrostatic interactions between the MLL site and peptides result in greater association rates when peptides bind to the MLL site. Consequently, when a dual-motif KIX binding protein (ie FOXO3a and p53 TAD) interacts with the KIX domain, the association process is mainly initiated by interactions between a KIX-binding motif and the MLL site.

ORCID

Yongqi Huang  <http://orcid.org/0000-0002-9463-8325>

REFERENCES

- [1] Ward JJ, Sodhi JS, McGuffin LJ, Buxton BF, Jones DT. Prediction and functional analysis of native disorder in proteins from the three kingdoms of life. *J Mol Biol.* 2004;337(3):635–645.
- [2] Peng Z, Mizianty MJ, Kurgan L. Genome-scale prediction of proteins with long intrinsically disordered regions. *Proteins.* 2014;82(1):145–158.
- [3] Lobley A, Swindells MB, Orengo CA, Jones DT. Inferring function using patterns of native disorder in proteins. *PLoS Comput Biol.* 2007;3(8):e162
- [4] Xie HB, Vucetic S, Iakoucheva LM, et al. Functional anthology of intrinsic disorder. 1. Biological processes and functions of proteins with long disordered regions. *J Proteome Res.* 2007;6(5):1882–1898.
- [5] Wright PE, Dyson HJ. Intrinsically disordered proteins in cellular signalling and regulation. *Nat Rev Mol Cell Biol.* 2015;16(1):18–29.
- [6] Liu ZR, Huang YQ. Advantages of proteins being disordered. *Protein Sci.* 2014;23(5):539–550.
- [7] DeForte S, Uversky VN. Not an exception to the rule: the functional significance of intrinsically disordered protein regions in enzymes. *Mol Biosyst.* 2017;13(3):463–469.
- [8] Uversky VN. p53 Proteoforms and intrinsic disorder: an illustration of the protein structure-function continuum concept. *Int. J Mol Sci.* 2016;17(11):1874
- [9] Van Roey K, Uyar B, Weatheritt RJ, et al. Short linear motifs: ubiquitous and functionally diverse protein interaction modules directing cell regulation. *Chem Rev.* 2014;114(13):6733–6778.
- [10] Ernst P, Wang J, Huang M, Goodman RH, Korsmeyer SJ. MLL and CREB bind cooperatively to the nuclear coactivator CREB-binding protein. *Mol Cell Biol.* 2001;21(7):2249–2258.
- [11] Campbell KM, Lumb KJ. Structurally distinct modes of recognition of the KIX domain of CBP by Jun and CREB. *Biochemistry.* 2002;41(47):13956–13964.
- [12] Zor T, De Guzman RN, Dyson HJ, Wright PE. Solution structure of the KIX domain of CBP bound to the transactivation domain of c-Myb. *J Mol Biol.* 2004;337(3):521–534.
- [13] Radhakrishnan I, Pérez-Alvarado GC, Parker D, Dyson HJ, Montminy MR, Wright PE. Solution structure of the KIX domain of CBP bound to the transactivation domain of CREB: a model for activator:coactivator interactions. *Cell.* 1997;91(6):741–752.
- [14] Goto NK, Zor T, Martinez-Yamout M, Dyson HJ, Wright PE. Cooperativity in transcription factor binding to the coactivator CREB-binding protein (CBP). The mixed lineage leukemia protein (MLL) activation domain binds to an allosteric site on the KIX domain. *J Biol Chem.* 2002;277(45):43168–43174.
- [15] Vendel AC, McBryant SJ, Lumb KJ. KIX-mediated assembly of the CBP-CREB-HTLV-1 tax coactivator-activator complex. *Biochemistry.* 2003;42(43):12481–12487.
- [16] De Guzman RN, Goto NK, Dyson HJ, Wright PE. Structural basis for cooperative transcription factor binding to the CBP coactivator. *J Mol Biol.* 2006;355(5):1005–1013.
- [17] Sugase K, Dyson HJ, Wright PE. Mechanism of coupled folding and binding of an intrinsically disordered protein. *Nature.* 2007;447(7147):1021–1025.
- [18] Gianni S, Morrone A, Giri R, Brunori M. A folding-after-binding mechanism describes the recognition between the transactivation domain of c-Myb and the KIX domain of the CREB-binding protein. *Biochem Biophys Res Commun.* 2012;428(2):205–209.
- [19] Arai M, Sugase K, Dyson HJ, Wright PE. Conformational propensities of intrinsically disordered proteins influence the mechanism of binding and folding. *Proc Natl Acad Sci USA.* 2015;112(31):9614–9619.
- [20] Toto A, Camilloni C, Giri R, Brunori M, Vendruscolo M, Gianni S. Molecular recognition by templated folding of an intrinsically disordered protein. *Sci Rep.* 2016;6:21994
- [21] Lee CW, Arai M, Martinez-Yamout MA, Dyson HJ, Wright PE. Mapping the interactions of the p53 transactivation domain with the KIX domain of CBP. *Biochemistry.* 2009;48(10):2115–2124.
- [22] Wang F, Marshall CB, Yamamoto K, et al. Structures of KIX domain of CBP in complex with two FOXO3a transactivation domains reveal promiscuity and plasticity in coactivator recruitment. *Proc Natl Acad Sci USA.* 2012;109(16):6078–6083.
- [23] Dyson HJ, Wright PE. Coupling of folding and binding for unstructured proteins. *Curr Opin Struct Biol.* 2002;12(1):54–60.
- [24] Zhou HX, Pang X, Lu C. Rate constants and mechanisms of intrinsically disordered proteins binding to structured targets. *Phys Chem Chem Phys.* 2012;14(30):10466–10476.
- [25] Webb B, Sali A. *Comparative Protein Structure Modeling Using Modeller.* *Current Protocols in Bioinformatics.* John Wiley & Sons, Inc, 2014: 5.6.1–5.6.32
- [26] Hess B, Kutzner C, Dvd S, Lindahl E. GROMACS 4: algorithms for highly efficient, load-balanced, and scalable molecular simulation. *J Chem Theory Comput.* 2008;4(3):435–447.
- [27] Lindorff-Larsen K, Piana S, Palmo K, et al. Improved side-chain torsion potentials for the Amber ff99SB protein force field. *Proteins.* 2010;78(8):1950–1958.
- [28] Alsallaq R, Zhou H-X. Electrostatic rate enhancement and transient complex of protein-protein association. *Proteins.* 2008;71(1):320–335.
- [29] Qin S, Pang X, Zhou HX. Automated prediction of protein association rate constants. *Structure.* 2011;19(12):1744–1751.
- [30] Pang X, Zhou KH, Qin S, Zhou HX. Prediction and dissection of widely-varying association rate constants of actin-binding proteins. *PLoS Comput Biol.* 2012;8(10):e1002696
- [31] Pang X, Zhou HX. Distinct mechanisms of a phosphotyrosyl peptide binding to two SH2 domains. *J Theor Comput Chem.* 2014;13(3): 1440003
- [32] Pang X, Zhou HX. Mechanism and rate constants of the Cdc42 GTPase binding with intrinsically disordered effectors. *Proteins.* 2016;84(5):674–685.
- [33] Clementi C, Nymeyer H, Onuchic JN. Topological and energetic factors: what determines the structural details of the transition state ensemble and “en-route” intermediates for protein folding? An investigation for small globular proteins. *J Mol Biol.* 2000;298(5): 937–953.
- [34] Stefan W, Hue Sun C. Conformational entropic barriers in topology-dependent protein folding: perspectives from a simple native-centric polymer model. *J Phys: Condens Matter.* 2006;18(14):S307
- [35] Ganguly D, Zhang W, Chen J. Electrostatically accelerated encounter and folding for facile recognition of intrinsically disordered proteins. *PLoS Comput Biol.* 2013;9(11):e1003363
- [36] Kaya H, Chan HS. Solvation effects and driving forces for protein thermodynamic and kinetic cooperativity: how adequate is native-centric topological modeling?. *J Mol Biol.* 2003;326(3):911–931.
- [37] Liu ZR, Chan HS. Desolvation is a likely origin of robust enthalpic barriers to protein folding. *J Mol Biol.* 2005;349(4):872–889.

- [38] Huang YQ, Liu ZR. Kinetic advantage of intrinsically disordered proteins in coupled folding-binding process: a critical assessment of the “fly-casting” mechanism. *J Mol Biol.* 2009;393(5):1143–1159.
- [39] Shammass SL, Travis AJ, Clarke J. Allostery within a transcription coactivator is predominantly mediated through dissociation rate constants. *Proc Natl Acad Sci USA.* 2014;111(33):12055–12060.
- [40] Shoemaker BA, Portman JJ, Wolynes PG. Speeding molecular recognition by using the folding funnel: the fly-casting mechanism. *Proc Natl Acad Sci USA.* 2000;97(16):8868–8873.
- [41] Umezawa K, Ohnuki J, Higo J, Takano M. Intrinsic disorder accelerates dissociation rather than association. *Proteins.* 2016;84(8):1124–1133.
- [42] Lacy ER, Filippov I, Lewis WS, et al. p27 binds cyclin-CDK complexes through a sequential mechanism involving binding-induced protein folding. *Nat Struct Mol Biol.* 2004;11(4):358–364.
- [43] Zhang W, Ganguly D, Chen J. Residual structures, conformational fluctuations, and electrostatic interactions in the synergistic folding of two intrinsically disordered proteins. *PLoS Comput Biol.* 2012;8(1):e1002353
- [44] Tsai MY, Zheng W, Balamurugan D, et al. Electrostatics, structure prediction, and the energy landscapes for protein folding and binding. *Protein Sci.* 2016;25(1):255–269.
- [45] Chu WT, Clarke J, Shammass SL, Wang J. Role of non-native electrostatic interactions in the coupled folding and binding of PUMA with Mcl-1. *PLoS Comput Biol.* 2017;13(4):e1005468.

SUPPORTING INFORMATION

Additional Supporting Information may be found online in the supporting information tab for this article.

How to cite this article: Huang Y, Gao M, Yang F, Zhang L, Su Z. Deciphering the promiscuous interactions between intrinsically disordered transactivation domains and the KIX domain. *Proteins.* 2017;85:2088–2095. <https://doi.org/10.1002/prot.25364>